

is explored. The IR results indicate that the rate constant for the epoxy and primary amine reaction depends on the diamine molecular weight. The rate constant increases as the molecular weight of the diamines decreases. However, the molecular weight dependence of the rate constant by itself can only provide a partial explanation for the formation of the observed structure. The DSC results indicate that the samples containing two diamines of different molecular weight are single-phase materials.

The scattering results of the acetone- d_6 swollen epoxies can be quantitatively fitted with one Lorentzian function, and the correlation length is about 10 Å regardless of the diamine size. However, the high value of χ' needed to fit the data again indicates the heterogeneous nature of the gel structure; the χ' obtained is found to be greater than 0.5. Once again, χ' shall not be regarded simply as the interaction parameter between acetone- d_6 and the epoxy network chains. Rather, it is an index denoting the extent of heterogeneity of solvent distribution throughout the specimen. The heterogeneity of the network in terms of the spatial distribution of the cross-links can result in a high χ' value as observed.

The broad scattering maximum observed in the acetone- d_6 swollen epoxy containing an equal mole of D-2000 and D-230 diamines can be interpreted with a regularly alternating block structure in an intranetwork sense. Within an average network the D-230 and D-2000, diamine chains were situated in a regularly alternating fashion. A semiquantitative explanation is provided by using the

excluded-volume concept to account for the scattering maximum observed. However, the theoretical work is derived for a highly regular structure, the possible randomization of the regular alternating sequence is not included in this current treatment. Consequently, the fit between the calculated and the observed results is only marginal.

Acknowledgment. We are grateful to C. J. Glinka and J. Gotaas for their help in the neutron measurements. Two of the authors (Yang and Stein) would like to thank CU-MIRP for its financial support of this work.

Registry No. (D-230)(DER 332) (copolymer), 112320-38-4; neutron, 12586-31-1.

References and Notes

- (1) Wu, W.; Bauer, B. J. *Macromolecules* **1986**, *19*, 1613.
- (2) Benoit, H.; Wu, W.; Benmouna, M.; Mozer, B.; Bauer, B. J.; Lapp, A. *Macromolecules* **1985**, *18*, 986.
- (3) Bastide, J.; Duplessix, R.; Picotand, C.; Candau, S. *Macromolecules* **1983**, *17*, 83.
- (4) de Gennes, P.-G. *Scaling Concepts in Polymer Physics*; Cornell University Press: Ithaca, NY, 1979.
- (5) Benoit, H.; Benmouna, M. *Polymer* **1984**, *25*, 1059.
- (6) Cahn, J. W.; Hilliard, J. E. *J. Chem. Phys.* **1958**, *28*, 258.
- (7) Flory, P. J. *Principles of Polymer Chemistry*; Cornell University Press: Ithaca, NY, 1957.
- (8) Wu, W.; Bauer, B. J. *Polymer* **1986**, *27*, 169.
- (9) Fischer, E. W. *Pure Appl. Chem.* **1978**, *50*, 1319.
- (10) Davidson, N. S.; Richards, R. W.; Macconnachie, A. *Macromolecules* **1986**, *19*, 431.
- (11) Flory, P. J. *Proc. R. Soc. London, Ser. A* **1976**, *351*, 351.

Free Energy Change in Hydrophobic Interactions Involving a Polyelectrolyte and Ruthenium Tris(bipyridine). A Pulsed Laser Study

Anny Slama-Schwok and Joseph Rabani*

Energy Research Center and The Department of Physical Chemistry, The Hebrew University of Jerusalem, Jerusalem 91904, Israel. Received May 8, 1987; Revised Manuscript Received September 8, 1987

ABSTRACT: Comparison between the effects of inert salts on the distribution of $\text{Ru}(\text{bpy})_3^{2+}$ ions around three negative polyelectrolytes, poly(styrenesulfonate) (PSS), poly(vinyl sulfate) (PVS), and poly(acrylate) (PAA), is reported. Much higher ion concentrations are required in order to remove $\text{Ru}(\text{bpy})_3^{2+}$ from PSS, as compared to removal from a PVS or PAA. Attributing the difference between these systems to the effect of hydrophobic interactions in the PSS enables the calculation of the free energy change involved in the formation of $\text{Ru}(\text{bpy})_3^{2+}$ -PSS. The results show a definite distinction between $\text{Ru}(\text{bpy})_3^{2+}$ "inside" and "outside" the polymer, with no exchange during the lifetime of the excited state of the ruthenium tris(bipyridine), $\text{Ru}(\text{bpy})_3^{2+*}$. The $\text{Ru}(\text{bpy})_3^{2+}$ ions are located more deeply "inside" the PSS as compared with the PVS.

Introduction

Thermodynamic properties of hydrophobic bonds have been quantitatively treated in biological systems for many years. Thus, Klotz, Walker, and Pivan¹ investigated the binding of organic ions by proteins and separated the electrostatic interactions from the hydrophobic interactions between the aromatic rings. The additional affinity due to the hydrophobic interactions was estimated in this system as 0.52 kcal. Nemethy and Scheraga² calculated standard free energies for interactions between two side chains of proteins as ranging between -0.2 and 1.5 kcal/mol. Several aromatic ammonium salts were reported to

interact with anionic polyelectrolytes and with a neutral polymer by hydrophobic interactions.³⁻⁶ The thermodynamics of hydrophobic interactions in biological systems has been lately discussed in detail by Ben-Naim.⁷ Parmauro, Pelizzetti, and Diekmann⁸ investigated the separation of electrostatic and nonelectrostatic environmental effects in redox reactions involving osmium coordination compounds observed in micelle solutions. Hydrophobic interactions between hydrophobic segments of polyelectrolytes and photosensitizers, electron donors, and electron acceptors have been extensively investigated lately. Weber⁹ and Morishima et al.¹⁰⁻¹⁴ employed charged co-

polymers containing alternating and randomly distributed hydrophobic photosensitizers incorporated in the polymer chains. Hydrophobic interactions in homopolymers have also been reported. Poly(styrenesulfonate) (PSS) and the well-known photosensitizer $\text{Ru}(\text{bpy})_3^{2+}$ were investigated by means of cation-exchange resins and showed an unusually strong binding of $\text{Ru}(\text{bpy})_3^{2+}$ to PSS.¹⁵ Hydrophobic interactions have also been invoked in order to explain the reaction kinetics in several photochemical systems.¹⁶

In the present work we attempt to measure the free energy change of the hydrophobic interactions between $\text{Ru}(\text{bpy})_3^{2+}$ and PSS. This is achieved by comparison between the effects of inert ions on the distribution of $\text{Ru}(\text{bpy})_3^{2+}$ in aqueous solutions containing different polymers.

Experimental Section

Spectrofluorimetric measurements were carried out by using a Perkin-Elmer Model LS-5 spectrofluorimeter. The excitation wavelength was 437 nm. Emission spectra were recorded in the range 550–650 nm with a 1-cm cell. Typical $\text{Ru}(\text{bpy})_3^{2+}$ concentration was 3×10^{-5} M. Pulsed laser photolysis was carried out on a Molelectron Model DL-200 dye laser.¹⁷ The excitation was carried out at 437 nm with Molelectron 70355-1C12 dye. Emission was detected at 612 nm by using a Hamamatsu photomultiplier. A cutoff filter transparent above 550 nm was used to filter the emitted light. A neutral density filter was employed in order to reduce the laser pulse intensity. Usually, the laser intensity was reduced to $(1.5 \text{ or } 3.7) \times 10^{-7}$ einstein $\text{L}^{-1}/\text{pulse}$. A Tektronix Model 7912 AD digitizer was used. In a typical experiment the results of 128 pulses were averaged. The test cells, 1×1 cm, contained 3 mL of solution and were closed with a rubber septum and bubbled with ultrapure He. The solutions were used within 2 h to avoid significant air leakage.

Materials. The $\text{Ru}(\text{bpy})_3\text{Cl}_2$ product of K&K was twice recrystallized from water. Water was purified by distillation followed by passing through a Millipore ion-exchange system. $\text{K}_4\text{Fe}(\text{CN})_6$ (Merck) AR grade was used as received. Stock solutions were prepared in air-free water and kept in a syringe in the dark for not more than 1 day. MgSO_4 (Mallinckrodt, AR grade), NaCl (Merck, AR grade), and KCl (Baker, AR grade) were used without further purification. Helium was Matheson's 99.999%. Poly(acrylic acid) (PAA; acid form) (Aldrich, MW 250 000) was used as received. Poly(styrenesulfonate) (PSS) sodium salts (Polysciences, MW 70 000 and 500 000) were purified by dialysis of a solution containing 3% PSS (by weight) and 10^{-4} M EDTA against water. Poly(vinyl sulfate) (PVS) (Sigma, MW 250 000) was purified as described before.¹⁸

Results and Discussion

$\text{Ru}(\text{bpy})_3^{2+}$ has a well-known visible absorption (peaking at 452 nm) and emission (peaking at 610 nm) spectra. No effects of PVS and inert salts on the shapes of these spectra, or on the lifetime of the emission, are observed.¹⁹ We tested the effects of PSS, PVS, and PAA on the emission spectrum and lifetimes of the emitting excited state. The emission spectrum remains unchanged and is identical with that observed in polyelectrolyte-free water. The rate constant for natural decay, k_N , equals $(1.60 \pm 0.15) \times 10^6 \text{ s}^{-1}$ for both PAA and PVS. This value is the same as observed in water containing no polymer. Addition of PSS leaves the spectrum unchanged, but $k_N = (1.2 \pm 0.1) \times 10^6 \text{ s}^{-1}$ in this case. Addition of $\text{Fe}(\text{CN})_6^{4-}$ ions in the absence of polymer has a strong effect on the emission intensity and on the lifetime of $\text{Ru}(\text{bpy})_3^{2+}$, as ferrocyanide has been reported to behave as an efficient quencher in this system, $k_q = 3.3 \times 10^9 \text{ M}^{-1} \text{ s}^{-1}$ at ionic strength $\mu = 0.5$.²⁰ Since a negative polymer is expected to retard the rate of quenching of the excited $\text{Ru}(\text{bpy})_3^{2+}$ by ferrocyanide ions, we used the difference in reactivity in order to obtain information about the distribution of

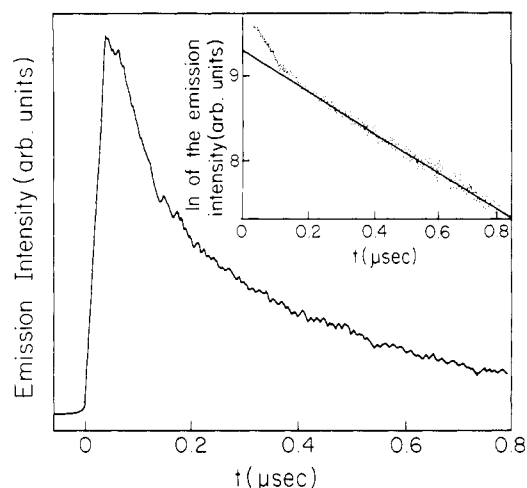


Figure 1. Typical computer trace representing the change of emission intensity with time after a laser pulse. Insert: the first-order plot, demonstrating the existence of two processes. 3×10^{-5} M $\text{Ru}(\text{bpy})_3^{2+}$, 3 mM PVS, 3 mM MgSO_4 , 1 mM $\text{K}_4\text{Fe}(\text{CN})_6$.

the $\text{Ru}(\text{bpy})_3^{2+}$ ions inside and outside the polymers' electric fields. When this method is used, the terms inside and outside are defined by the availability of excited $\text{Ru}(\text{bpy})_3^{2+}$ for quenching by ferrocyanide ions. Preliminary work was always carried out by the spectrofluorimetric method. However, since the addition of inert counterions may enhance the rate of $\text{Ru}(\text{bpy})_3^{2+}$ quenching by ferrocyanide within the polymer field, and retard this rate in the bulk, the steady-state emission intensity alone cannot be used as a criterion for the $\text{Ru}(\text{bpy})_3^{2+}$ distribution. We preferred the use of pulsed laser kinetics and followed the decay of emission at 612 nm. In the presence of a negatively charged polyelectrolyte, this decay has two parts (Figure 1). The fast decay represents the quenching of excited $\text{Ru}(\text{bpy})_3^{2+}$ by ferrocyanide ions in the bulk, while the slow decay represents the quenching inside the polymer field. The quenching rate constant of $\text{Ru}(\text{bpy})_3^{2+}$ by ferrocyanide ions, k_q , in the bulk varies with ionic strength as predicted by the Debye-Hückel equation, corresponding to an ionic charge product of 6. This result is reasonable since ion-pair formation may change the effective ionic charge. The experimental results are summarized in Table I. The salt effects on the quenching rates in the polyelectrolytes are relatively small. It can be seen from Table I that quenching rates increase considerably upon addition of salts in the cases of PVS and PVA. In contrast, no salt effect on the quenching rate is observed in the PSS solutions, even at very high ionic concentrations (e.g., 0.4 M NaCl). We explain this by the contribution of the hydrophobic interactions between the $\text{Ru}(\text{bpy})_3^{2+}$ and the aromatic groups of the PSS. This affects the distribution of $\text{Ru}(\text{bpy})_3^{2+}$ ions so that these ions are located nearer the polymer backbone, as compared with the Poisson distribution of the $\text{Ru}(\text{bpy})_3^{2+}$ ions as determined by the electric fields only (in PVA and PVS). The $\text{Ru}(\text{bpy})_3^{2+}$ in the PSS solutions is less available to react with the ferrocyanide quencher.

The fraction of emission which decays away in the fast part increases with the salt concentration, at a given polymer concentration. Typical results are presented in Figure 2, where the ratio of emission intensities in the fast and slow decays, respectively, is plotted against the inert counterion concentration. Note that the effects of the monovalent counterions present initially (K^+ from the PVS, PAA, and potassium ferrocyanide, Na^+ from PSS and PAA) are small in comparison with the effects of the

Table I
Effect of Inert Ions on the Quenching of $\text{Ru}(\text{bpy})_3^{2+}$ by $\text{Fe}(\text{CN})_6^{4-}$ ^a

polymer	[monomer], mM	salt	[salt], mM	$k_q(i)$ ^b
(A) In Polyelectrolyte Solutions				
PVS	0.6	MgSO ₄	6	13
PVS	1.5	MgSO ₄	3	8
PVS	3.0	MgSO ₄	3	7
PVS	3.0	MgSO ₄	6	9
PVS	3.0	MgSO ₄	12	12
PVS	1.0	KCl	30	6
PAA ^c	1.0	NaCl	5	11
PAA ^c	1.0	NaCl	10	13
PAA ^c	3.0	NaCl	10	7
PAA ^c	3.0	NaCl	30	32
PAA ^c	1.0	KCl	10	6
PAA ^c	1.0	KCl	20	8
PAA ^c	1.0	KCl	30	31
PAA ^d	0.4	NaCl	5	9
PAA ^d	1.2	NaCl	10	6
PAA ^d	1.2	NaCl	30	49
PAA ^d	1.5	KCl	20	11
(B) In the Absence of Polyelectrolytes				
	^e			
	MgSO ₄ ^e	0		380
		100		35
		0		320
	CsCl	4		220
	CsCl	5		180
	CsCl	8		140
	CsCl	15		120

^a $[\text{Ru}(\text{bpy})_3^{2+}] = 3 \times 10^{-5}$ M; $[\text{Fe}(\text{CN})_6^{4-}] = 1$ mM. ^b In units of $10^8 \text{ M}^{-1} \text{ s}^{-1}$. The rate constants are for the $\text{Ru}(\text{bpy})_3^{2+}$ inside the polymer. ^c Fully ionized by NaOH or KOH. ^d 60% ionized by NaOH or KOH. 40% neutralized by complexation with magnesium ions. ^e 0.1 mM ferrocyanide ions.

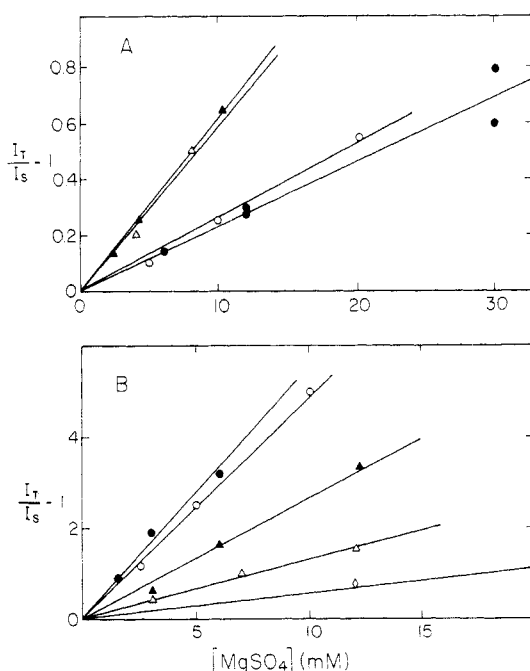


Figure 2. Typical plots of the ratios of emission intensities in the fast ($I_T - I_S$) and slow (I_S) decays. I_T is the initial intensity measured in Figure 1. I_S is the initial extrapolated intensity for the slower stage. Total $[\text{Ru}(\text{bpy})_3^{2+}]$ is 3×10^{-5} M. $[\text{Fe}(\text{CN})_6^{4-}]$ is 1 mM. Polymer concentrations are given in molarity of monomer units. (A) PSS present: \blacktriangle , 5×10^{-4} ; \triangle , 6×10^{-4} ; \bullet , 1×10^{-3} ; \circ , 3×10^{-3} . (B) PVS present: \bullet , 6×10^{-4} ; \circ , 1×10^{-3} ; \blacktriangle , 1.5×10^{-3} ; \triangle , 3×10^{-3} ; \diamond , 6×10^{-3} .

bivalent Mg^{2+} ions. Similar experiments in which the Mg^{2+} ions were replaced by the singly charged Na^+ or K^+ ions (as chlorides) were also carried out (not shown in Figure 2). In the case of PSS, the concentration of the initially

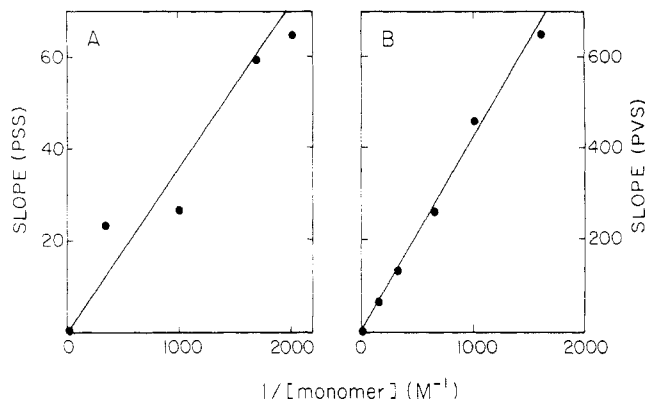
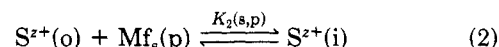
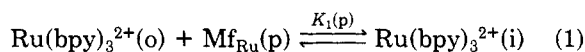


Figure 3. Typical plots of the slopes (Figure 2) vs $[\text{M}(\text{p})]^{-1}$. The experimental points represent the slopes from Figure 2.

present K^+ (counterion of $\text{Fe}(\text{CN})_6^{4-}$) and Na^+ (counterion of PSS) was small in comparison with the added sodium or potassium chlorides.

In PAA and PVS, the effect of KCl could be easily studied as K^+ was the only counterion. On the other hand, when Na^+ was added to PVS or to PAA, K^+ was also present (as a counterion of PVS and $\text{Fe}(\text{CN})_6^{4-}$), and its effect could not be neglected. In the data treatment we corrected for the K^+ effect by taking $[\text{Na}^+]$ as the sum of added $[\text{NaCl}]$ plus 1.6 times the $[\text{K}^+]$ present. The factor 1.6 is based on the work of Johah, Matheson, and Meisel,²¹ who found potassium 1.6-fold more effective than sodium in replacing other ions. The plots of the type shown in Figure 2 are typical to all three polymers at all inert ion concentrations used by us. As can be seen in Figure 2, the slopes of the straight lines usually decrease with increasing concentration of the polymer. A closer look reveals that the above slopes change linearly with the inverse of the polymer concentration as demonstrated in Figure 3. The results are independent of the polymer chain length (tested by comparison between PSS with molecular weights 70 000 and 500 000).

The observation of two decay processes, separated in time (Figure 1), attributed to the quenching of the excited $\text{Ru}(\text{bpy})_3^{2+}$ outside and inside the polymer, respectively, indicates that the quenching reactions are fast as compared with the rate of exchange of $\text{Ru}(\text{bpy})_3^{2+}$ between the polymer and the bulk. Had the exchange rate been faster than the fast quenching rate, only one decay stage would have been observed. It is also unlikely that the exchange rate is slower than the fast quenching rate but faster than the slow quenching rate. In such a case, two stages separated in time would have resulted, enabling the measurement of $\text{Ru}(\text{bpy})_3^{2+}$ distributions inside and outside the polymer fields. However, in such a case, the slower quenching rate would have been determined by the rate of exchange and would be independent of $[\text{Fe}(\text{CN})_6^{4-}]$, which is contrary to the observation that the rates of both decay processes increase with increasing $[\text{Fe}(\text{CN})_6^{4-}]$. The effect of inert counterions can be described in terms of the equilibrium reactions 1 and 2. The subscripts o and i



represent the solutes outside and inside the polymer, respectively. $\text{Mf}_x(\text{p})$ represents a segment of the polymer p available for the condensation of one counterion of the type x. The equilibrium constants of the right-hand side of eq 1 and 2 are expressed as $[\text{ion}(\text{i})]/([\text{ion}(\text{o})][\text{Mf}_x(\text{p})])$. $[\text{Mf}_x(\text{p})]$ equals $[\text{M}(\text{p})]/z$, where $[\text{M}(\text{p})]$ is the polymer

Table II
Summary of $(2K_2(s,p))/K_1(p)$ for the Various Polymers

salt	$(2K_2(s,PVS))/K_1(PVS)$	$(2K_2(s,PSS))/K_1(PSS)$	$(2K_2(s,PAA))/K_1(PAA)$
NaCl	$(5.0 \pm 1.5) \times 10^{-2}$	$(7.0 \pm 2.0) \times 10^{-3}$	$(1.1 \pm 0.3) \times 10^{-1}$
KCl	$(6.0 \pm 1.5) \times 10^{-2}$		$(7 \pm 1) \times 10^{-2}$
MgSO ₄	$(4.2 \pm 0.4) \times 10^{-1}$	$(3.6 \pm 0.6) \times 10^{-2}$	

concentration in monomer units and z is the ionic charge. From eq 1 and 2 one can easily obtain eq 3

$$[\text{Ru}(\text{bpy})_3^{2+}(\text{o})][\text{S}^{z+}(\text{i})]/([\text{Ru}(\text{bpy})_3^{2+}(\text{i})][\text{S}^{z+}(\text{o})]) = \frac{2K_2(s,p)}{K_1(p)z} \quad (3)$$

In deriving this equation, it is assumed that the capacity of a given polymer with respect to the counterions is determined by the charge only. In the case of $\text{Ru}(\text{bpy})_3^{2+}$, which is a relatively large ion, this may not be exactly the case. Any deviations, e.g., due to steric hindrance, will be included in the equilibrium constant. If $[\text{Ru}(\text{bpy})_3^{2+}] \ll [\text{M}(p)] \ll [\text{S}^{z+}]$, the electrical balance equation

$$[\text{M}(p)] = [\text{M}_f] + z[\text{S}^{z+}(\text{i})] + 2[\text{Ru}(\text{bpy})_3^{2+}(\text{i})]$$

($[\text{M}_f]$ is the concentration of the free monomer units available for condensation of counterions) can be reduced to $[\text{M}(p)] = z[\text{S}^{z+}(\text{i})]$ since under such conditions both $[\text{M}_f]$ and $[\text{Ru}(\text{bpy})_3^{2+}(\text{i})]$ are relatively small. Under the same conditions, $[\text{S}^{z+}(\text{o})] = [\text{S}^{z+}]$ (the total inert ions' concentration). Thus, eq 3 can be revised to 3'

$$[\text{Ru}(\text{bpy})_3^{2+}(\text{o})]/[\text{Ru}(\text{bpy})_3^{2+}(\text{i})] = \frac{(2K_2(s,p)[\text{S}^{z+}])}{(K_1(p)[\text{M}(p)])} \quad (3')$$

The measured values of $(I_T/I_S)-1$ (Figure 2) represent the ratio on the left-hand side of eq 3'. The linear plots observed in Figure 3 agree with this interpretation. Note that reasonable straight lines are obtained only when $[\text{Ru}(\text{bpy})_3^{2+}]$ is very small in comparison with $[\text{M}(p)]$ and the inert salt is in large excess over $[\text{M}(p)]$. The slopes of the straight lines plotted in Figure 2 equal $2K_2(s,p)/(K_1(p)[\text{M}(p)])$. These slopes vary linearly with $1/[\text{M}(p)]$, as expected from eq 3' (Figure 3). The slopes of Figure 3 are equal to $2K_2(s,p)/K_1(p)$. In Table II we summarize these constants, as measured in PVS, PAA, and PSS, using MgSO_4 , KCl, or NaCl as inert salts.

The equilibrium constants are related to the standard free energy changes as follows:

$$\Delta G_1^\circ(p) = -RT \ln (K_1(p)); \quad \Delta G_2^\circ(s,p) = -RT \ln K_2(s,p)$$

Let us now divide $\Delta G_1^\circ(\text{PSS})$ into two terms. One term is the free energy change due to the electrostatic interactions (e), and the second is the free energy change due to the hydrophobic interactions (h), namely:

$$\Delta G_1^\circ(\text{PSS}) = \Delta G_1^\circ(\text{PSS})_e + \Delta G_1^\circ(\text{PSS})_h = -RT \ln (K_1(\text{PSS})_e K_1(\text{PSS})_h)$$

Thus

$$[\Delta G_2^\circ(s,\text{PSS}) - \Delta G_1^\circ(\text{PSS})] - [\Delta G_2^\circ(s,\text{PVS}) - \Delta G_1^\circ(\text{PVS})] = -RT \ln \frac{(K_2(s,\text{PSS})K_1(\text{PVS}))}{(K_1(\text{PSS})_e K_1(\text{PSS})_h K_2(s,\text{PVS}))} \quad (4)$$

Let us now introduce $(K_1(\text{PSS})_e)/K_2(s,\text{PSS}) = K_1(\text{PVS})/K_2(s,\text{PVS})$. This assumption means that the distribution of the inert counterions inside and outside the polymer, relative to the distribution of $\text{Ru}(\text{bpy})_3^{2+}$, does not depend on the nature of the polymer as long as the interactions are purely electrostatic. The justification for

this under our conditions will be given later. Equation 4 is now simplified to eq 5, where $\Delta G^\circ(h)$ is the standard

$$-\Delta G^\circ(h) = RT \ln (K_1(\text{PSS})_h) \quad (5)$$

free energy change due to the hydrophobic interactions between the $\text{Ru}(\text{bpy})_3^{2+}$ and PSS, separated from the electrostatic interactions. Our results yield $\Delta G^\circ(h) = 1.5 \pm 0.2$ and 1.2 ± 0.3 kcal/mol, based on the experiments with Mg^{2+} and Na^+ , respectively. If an ion is considered as a point charge, and only electrostatic interactions are important, then the distribution of different ions possessing the same charge in a polyelectrolyte solution must be independent of the exact nature of the ion. This situation implies that, in the absence of any interactions other than the electrostatic interactions with the polymer, $K_1(p)$ must equal $K_2(s,p)$ for all ions possessing the same charges. Jonah, Matheson and Meisel²¹ measured specificity constants for mono- and divalent ions, using copper ions as reference. Their work shows that among ions possessing the same charge the larger ions are somewhat more effective in removing other counterions. This may be connected with ionic hydration sphere effects.²² The ratio of the equilibrium constants in the PVS system (Table II) shows somewhat stronger interactions between PVS and $\text{Ru}(\text{bpy})_3^{2+}$ as compared to Mg^{2+} ions. The value of the constants' ratio is in the range reported by Jonah, Matheson, and Meisel²¹ for simple ions. Therefore, we conclude that only small, if any, hydrophobic interactions exist between $\text{Ru}(\text{bpy})_3^{2+}$ ions and PVS.

PVS and PSS have somewhat different charge densities. The question arises whether the charge density may be a major factor in determining the relative distributions of the different counterions, and thus introduce an uncertainty in our free energy determination of the hydrophobic interactions. In order to test this, we used PAA. When fully ionized (neutralization of the poly(acrylic acid) by KOH), it has a charge density similar to that of PVS. The charge density can be reduced by the addition of Mg^{2+} ions, which form a stable complex with the polycarboxylic entities. (We conclude this by analogy with simple bicarboxylic anions). Upon addition of appropriate concentrations of magnesium ions, we were able to control the charge density. The effect of K^+ ions on the "free" polyelectrolyte and on the magnesium-containing polymer with 40% of the charge neutralized is similar (Table I). This indicates that the formal charge density of the polymer affects only little, if at all, the relative distribution of different ions inside and outside the polymer field. The results in PAA and PVS are similar when K^+ is used as a counterion. Na^+ is more effective in removing $\text{Ru}(\text{bpy})_3^{2+}$ from PAA as compared to PVS, apparently due to complex formation between the sodium ions and PAA.

Conclusions

The free energy change measured for the hydrophobic interactions between $\text{Ru}(\text{bpy})_3^{2+}$ and PSS is in the same range as the free energies of micelle formations.²³ This supports the interpretations of the previous works, which were based on qualitative considerations. It is interesting that eq 3', which is only approximately correct, is obeyed over a considerable range of concentrations. In varying the conditions, one has to consider the effect of inert ions not only on replacing the $\text{Ru}(\text{bpy})_3^{2+}$ ions but also in creating an opposite ionic atmosphere, which affects the electrostatic potential around the polymer. This effect is minimized if we use a large excess of ions that have the same charge as the $\text{Ru}(\text{bpy})_3^{2+}$. Under such conditions the total ionic atmosphere at the polymer apparently varies only relatively little.

These requirements are not exactly fulfilled when the monovalent ions are used. Although in our systems we did not observe very large deviations as observed previously,²¹ we consider the Mg^{2+} results more reliable.

Acknowledgment. We are indebted to S. Baer for helpfull discussions. This work was supported by the Israel-USA BNSF and by the Balfour Foundation, Israel.

Registry No. PSS, 9080-79-9; PVS, 25191-25-7; PAA, 9003-01-4; $Ru(bpy)_3^{2+}$, 15158-62-0; $K_4Fe(CN)_6$, 13943-58-3; $MgSO_4$, 7487-88-9; KCl, 7447-40-7; NaCl, 7647-14-5.

References and Notes

- (1) Klotz, I. M.; Walker, F. M.; Pivan, R. B. *J. Am. Chem. Soc.* **1946**, *68*, 1486.
- (2) Nemethy, G.; Scheraga, H. A. *J. Phys. Chem.* **1962**, *66*, 1773.
- (3) Gregor, H. P.; Frederick, M. J. *Polym. Sci.* **1957**, *23*, 451.
- (4) Turro, N. J.; Pierola, I. F. *J. Phys. Chem.* **1983**, *87*, 2420.
- (5) Miyamoto, S. *Macromolecules* **1981**, *14*, 1054.
- (6) Chen, C.-H.; Berns, D. S. *J. Phys. Chem.* **1977**, *81*, 125.
- (7) Ben-Naim, A. *Topics in Molecular Pharmacology*; Burgan, A. S. V., Roberts, G. C. K., Eds.; Elsevier: Amsterdam, 1983.
- (8) Paramauro, E.; Pelizzetti, E.; Dickmann, S.; Frahm, J. *Inorg. Chem.* **1982**, *21*, 2432.
- (9) Webber, S. E. *Macromolecules* **1986**, *19*, 1658.
- (10) Morishima, Y.; Kobayashi, T.; Nozakura, S. I. *J. Phys. Chem.* **1985**, *89*, 4081.
- (11) Morishima, Y.; Kitani, T.; Kobayashi, T.; Saeki, Y.; Nozakura, S. I.; Ohno, T.; Kato, S. *Photochem. Photobiol.* **1985**, *42*, 457.
- (12) Morishima, Y.; Itoh, Y.; Nozakura, S.-I.; Ohno, T.; Kato, S. *Macromolecules* **1984**, *17*, 2264.
- (13) Itoh, Y.; Morishima, Y.; Nozakura, S. *J. Polym. Sci., Polym. Chem. Ed.* **1982**, *20*, 467.
- (14) Morishima, Y.; Itoh, Y.; Nozakura, S.-I. *Chem. Phys. Lett.* **1982**, *91*, 258.
- (15) Kurimura, Y.; Yokota, H.; Shigehara, K.; Tsuchida, E. *Bull. Chem. Soc. Jpn.* **1982**, *55*, 55.
- (16) Sassoon, R. E.; Gershuni, S.; Rabani, J. *J. Phys. Chem.* **1985**, *89*, 1937.
- (17) Lougnot, D.; Dolan, G.; Goldstein, C. R. *J. Phys. E.* **1979**, *12*, 1051.
- (18) Breslow, D.; Kutner, K. *J. Polym. Sci.* **1958**, *27*, 295.
- (19) Jonah, C. D.; Matheson, M. S.; Meisel, D. *J. Phys. Chem.* **1979**, *83*, 257.
- (20) Juris, A.; Gandolfi, M. T.; Manfrine, M. F.; Balzani, V. *J. Am. Chem. Soc.* **1976**, *98*, 1047.
- (21) Jonah, C. D.; Matheson, M. S.; Meisel, D. *J. Phys. Chem.* **1977**, *81*, 1805.
- (22) Ise, N. *J. Polym. Sci., Polym. Symp.* **1978**, *62*, 205.
- (23) Fendler, J. H.; Fendler, E. J. *Catalysis in Micellar and Macromolecular Systems*; Academic: New York, 1975.

Whole-Pattern Approach to Structure Refinement Problems of Fibrous Materials. Application to Isotactic Polypropylene

A. Immirzi* and P. Iannelli

Dipartimento di Fisica, Università di Salerno, I-84100 Salerno, Italy.

Received February 25, 1987; Revised Manuscript Received September 18, 1987

ABSTRACT: Following up an idea developed in a previous paper, the crystal structure of the α form of isotactic polypropylene (IPP) has been refined by a least-square fitting procedure by using X-ray diffraction fiber data and considering the fiber spectrum as a whole. This approach represents an extension of the Rietveld method from the one-dimensional case (powders) to a two-dimensional case (fibers). In spite of structure complexity, low resolution, and reflection overlap, well-distinguishable fits have been obtained by considering the two structure models $P2_1/c$ and $C2/c$ which are very closely related to each other. A reliable chain model of 3_1 symmetry was obtained having C-C-C chain angles of 116.9° and 112.4° , chain torsion angles of 178° and 59° , and methyl-to-chain valence angles of 108.2° .

Introduction

In a preceding paper¹ we have discussed the possibility of performing crystal structure refinements from fiber diffraction data by using, instead of "integrated" diffraction intensities, the "whole diffraction pattern", so extending the Rietveld's method^{2,3} from the powder to the fiber case. The diffraction pattern as a whole can be digitized by using the photographic technique and a photoscanner instrument.

The advantage of the whole-pattern method against the traditional one is that the problem of reflection overlap is removed. Although in fibers overlap is less troublesome than in powders since it takes place only within each layer line, large lattice constants, low symmetry, and wide peak broadening make the problem serious. In the present case, for instance, from 4 to 8 reflections do contribute for at least 20% of their maximum weight to the equatorial points between $\vartheta = 25^\circ$ and $\vartheta = 35^\circ$ (twice as many in the upper level lines), and yet above $\vartheta = 10^\circ$ there are no points without any contribution. Among the overlapped reflections, of course, only a few are "intense"; for a quantitative treatment it is important, however, to consider all reflections, not only the intense.

In order to implement fiber whole-pattern refinement procedures, it is necessary to choose suitable profile

functions for expressing the distribution of diffracted intensity. While in the powder case a one-variable function is needed (the profile versus the diffraction Bragg angle 2ϑ), in the fiber case two-variable functions are required. In a preceding article¹ we have shown that in the case of the α form of isotactic polypropylene (IPP), X-ray radiation and photographic technique; Gaussian profile functions are adequate for expressing the intensity distribution both in the increasing Bragg angle direction and for a constant Bragg angle direction. On this basis a whole-pattern structure refinement for the same polymer has been carried out by considering, alternatively, the $C2/c$ structural model by Natta and Corradini⁴ and the $P2_1/c$ model by Mencick.⁵ The two fits are compared and discussed in this paper.

In the present study we have also combined the fiber whole-pattern approach with constrained refinement so considerably reducing the number of structural unknowns. The procedure applied is closely related to that used in powder whole-pattern studies.⁶⁻⁹

Experimental Section

The sample of IPP used in this study (the same used in the former work¹) was stretched at 140°C and annealed at 140°C for 3 h. The X-ray fiber diffraction pattern (Cu $K\alpha$ radiation)